Paclitaxel-Loaded and Folic Acid Modified PLGA Nanomedicine with Glutathione-Response for the Treatment of Lung Cancer

Zhanxia Zhang (zhanxiazhang2014@163.com)
Shanghai University of Traditional Chinese Medicine
Wang Yao
Shanghai University of Traditional Chinese Medicine
Jialiang Yao
Shanghai University of Traditional Chinese Medicine
Fangfang Qian
Shanghai University of Traditional Chinese Medicine
Zujun Que
Shanghai University of Traditional Chinese Medicine
Pan Yu
Shanghai University of Traditional Chinese Medicine
Tianle Luo
Shanghai University of Traditional Chinese Medicine
Dan Zheng
Shanghai University of Traditional Chinese Medicine
Jianhui Tian
Anhui University of Traditional Chinese Medicine

Research

Keywords: anticancer nanomedicine, stimuli response, targeted delivery, lung cancer, biodegradation

Posted Date: May 29th, 2020

DOI: https://doi.org/10.21203/rs.3.rs-30586/v1

Abstract

Targeted delivery and smart response of nanomedicine hold great promise to improve the therapeutic efficacy and alleviate the side effects of chemotherapy agents in cancer treatment. While a few research systems about organic nanomedicines with these properties have limited the development prospect of nanomedicines. In the present study, folic acid (FA) targeted delivery and GSH (glutathione) smart responsive nanomedicine was rationally designed for paclitaxel (PTX) delivery in the treatment of lung cancer. Compared with other stimuli responsive nanomedicines, this nano-carrier was not only sensitive to biologically relevant GSH for on demand drug release but also biodegradable into biocompatible by products after fulfilling its delivering task. The nanomedicine can firstly enter into tumor cells via FA and its receptor mediated endocytosis. After lysosomes escape, the PLGA (poly(lactic-co-glycolic acid) nanomedicine was triggered by the higher level of GSH and released its cargo in tumor microenvironment. *In vitro* and *in vivo* results revealed that the PLGA nanomedicine not only can inhibit the proliferation and promote the apoptosis of lung cancer cells greatly, but also possesses less toxic side effects when compared with free PTX. Therefore, the proposed drug delivery system demonstrates the encouraging potential for multifunctional nano-platform applicable to enhance the bioavailability and reduce the side effects of chemotherapy agents.

Introduction

Lung cancer is the malignant tumor with the highest morbidity (12%~13%) and mortality (22 ~ 24%) [1, 2]. Although surgical resection represents curative treatments for early stage of lung cancer, most patients with advanced lung cancer are not permissible to surgical resection and have to mainly rely on traditional radiation and/or chemotherapy [3]. The main chemotherapy agents include platinum complexes, paclitaxel, doxorubicin, decitabine, etc. [4] Paclitaxel (PTX) is a secondary metabolite extracted from the bark of yew. By promoting tubulin polymerization and inhibiting depolymerization as well as maintaining tubulin stability, PTX can accumulate a large number of tubules in cells to inhibit mitosis of tumor cells, so as to achieve the purpose of tumor inhibition [5, 6]. On one hand, PTX has outstanding anticancer effect. On the other hand, its toxic side effects are obvious, such as anaphylaxis from its solvent (polyoxyethylene castor oil), myelosuppression, neurotoxicity and cardiovascular toxicity, etc. [7] Hence, how to reduce PTX toxicity and side effects is an urgent problem to be solved. To reduce its toxic side effects, scientists developed a series of PTX nanomedicines, such as albumin-bound PTX (Abraxane) and liposome-entrapped PTX (LEP), etc. [8] Although these nanomedicines reduce the toxic side effects of PTX, a new generation of nanomedicines should have the properties of tumor microenvironmental response and targeted delivery to improve their therapeutic effect.

Nanomedicines have the advantage of EPR (enhanced permeability and retention), targeted delivery, stimuli response, long blood circulation time, embedding hydrophobic agents, penetrating body barrier (blood-brain barrier), etc. [9, 10] The past decades have witnessed the tremendous development of nanomedicines in the treatment of various cancers. At present, the representatives of nanomedicine are liposomal doxorubicin (Doxil), albumin-bound PTX (Abraxane), vincristine sulfate liposomes injection

(Marqibo), etc. [11, 12] Recently, for the development of a new generation nanomedicines, targeted delivery and tumor microenvironmental response have attracted wide attentions due to the reduction of side effects and the improvement of anti-cancer efficacy [13, 14]. For the targeted delivery of nanomedicines, the usual method is the modification of targeted molecules on the surface of nanomedicine, which include small molecules (FA, lectins, etc.), peptides, antibodies and nucleic acid aptamers, etc. [15–17] Among them, the overexpression of the folate receptor (FR) in a variety of malignant tumors, along with its limited expression in healthy tissues, makes FA an attractive tumor-specific targeted molecule. [18] For smart response, both external (including light, magnetic field, ultrasound, etc.) and internal (such as pH, temperature, enzyme, redox potential, etc.) stimuli have been intensively utilized to trigger the release of anticancer agents from nanomedicines in tumor microenvironments [19–21]. Among these reported stimuli, redox potential has attracted much attention due to the uniquely heterogeneous redox potential gradient in tumor microenvironment, such as over-expressed GSH and ROS (reactive oxygen species), etc. [22] Some studies have reported that the levels of GSH in tumors sites are generally higher than normal tissue for eliminating the high ROS level in tumor microenvironment, thus GSH is considered as a promising trigger for constructing smart responsive nanomedicines [23]. In general, most GSH responsive nanomedicines contain S-S (disulfide), Se-Se (diselenide) or thioether succinimide bonds. [24, 25]. Despite the remarkable advances in targeted delivery and controlled release of nanocarriers, there are a few reports on organic nanomedicines with these properties significantly restricts the development of nanomedicines.

In this study, we constructed a FA modified PLGA-SS-PEG (polyethylene glycol) nanomedicine for the targeted delivery of PTX, which contains disulfide bonds that can be degraded in a controlled manner by the high level of GSH in tumor microenvironment (Fig. 1). Briefly, the nanomedicine firstly entered into tumor cell through FA and its receptor mediated endocytosis. After lysosomes escape, the anticancer agent PTX was released from the PLGA nanomedicine through the smart response of GSH. *In vitro* and *in vivo* results indicated that the PLGA nanomedicine can significantly inhibit the proliferation and promote the apoptosis of lung cancer cells. Therefore, the PLGA nanomedicine not only relieved the toxic and side effects but also promoted the therapeutic efficacy of anticancer agent greatly. Importantly, the biodegradable nanomedicine with the merits of targeted delivery and smart response possesses a good application prospect in the field of nanomedicines.

Materials And Methods

Materials

Lactide (LA), glycolide (GA), 2,2-dithiodiethanol, PEG-bis(carboxymethyl), tin(II) 2-ethylhexanoate and 2-hydroxyethyl disulfide were purchased from Sigma. Other organic solvents used in this paper are all analytical pure. Folic acid (FA), poly(vinyl alcohol) (PVA), paclitaxel (PTX), nile red (NR) and reduced glutathione (r-GSH) were purchased from Aladdin. GSH and GSSG assay kit was purchased from Beyotime Biotechnology. Cleaved-caspase 3 and Ki-67 antibody were purchased from Abcam. The CCK-8 (cell counting kit-8) was purchased from MedChemExpress. Annexin V FITC Apoptosis Kit was purchased

from BD Biosciences. Alanine transaminase (ALT), aspartate aminotransferase (AST) and creatinine (CRE) activity assay kits were purchased from NanJing JianCheng Bioengineering Institute.

Synthesis of PLGA-SS-PEG-FA polymer materials

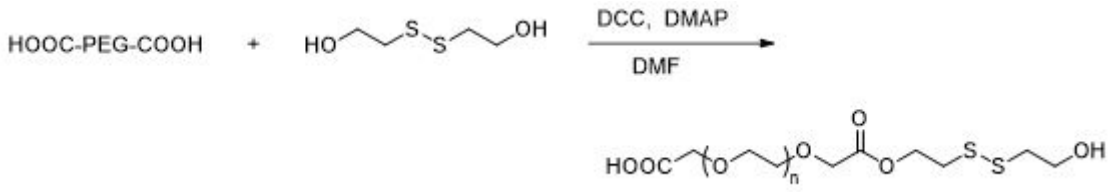

In a Schlenk flask, 2,2-dithiodiethanol (1 eq) was dissolved in DMF (N,N-dimethylformamide), followed by DCC (dicyclohexylcarbodiimide, 10 eq) and DMAP (4-dimethylaminopyridine, 0.2 eq). HOOC-PEG-COOH polymer (1 eq) was then added and the reaction was stirred at 30 ℃ for 24 hour. The reaction mixture was then concentrated on a rotary evaporator and the product was purified by precipitation in diethyl ether to get HOOC-PEG-SS-OH.

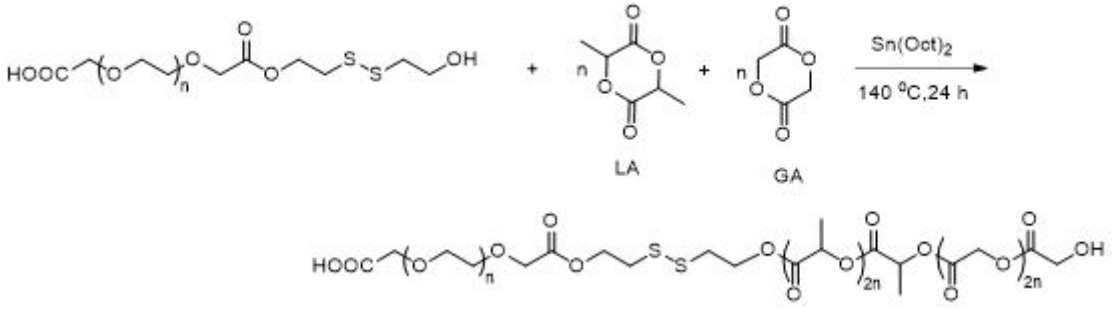

Ring opening polymerization of LA, GA was carried out using HOOC-PEG-SS-OH as initiator in the presence of tin(II) 2-ethylhexanoate as catalyst. Weighed amount of LA, GA was added in a Schlenk flask kept at 140 ℃. 2-Hydroxyethyl disulfide and tin(II) 2-ethylhexanoate was added to the Schlenk flask and reaction mixture was allowed to stir at 140 ℃ for 24 h under a N_2 flow. Resulting viscous solution was diluted with chloroform, and the product was purified by precipitation in diethyl ether to get HOOC-PEG-SS-PLGA.

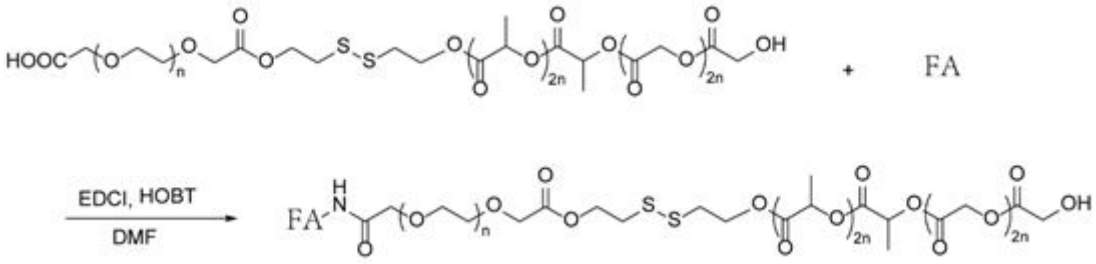

In a Schlenk flask, HOOC-PEG-SS-PLGA was dissolved in DMF, followed by EDCI and HOBT. FA was then added and the reaction was stirred at 30 °C for 72 h. The resulting products were purified and lyophilized to give product PLGA-SS-PEG-FA. The structure was identified by H1-NMR spectroscopy (Figure S1 in Supporting Information).

Preparation of PTX-loaded PLGA nanomedicine

The solvent volatilization method [22], with slight modification, was used to synthesize the nanomedicine used in this study. First, 100 mg of PLGA-SS-PEG-FA polymer and 5 mg of PTX or nile Red (NR) were fully dissolved in chloroform (0.5 ml) and added to 10 ml of PBS (phosphate buffer saline) containing 1% of PVA. Second, the suspension was mixed thoroughly using an ultrasonic emulsification (100 W) on ice bath for 2 minutes. The solution was then placed on a rotary evaporator and the dichloromethane was evaporated by stirring overnight. Finally, the nanomedicine was collected by centrifugation to remove the unloaded drug at 5000 rmp for 10 minutes and washed twice with ultrapure water using a centrifuge at room temperature. Similarly, the blank PLGA nanoparticles (NPs) were synthesized in the same way, except the addition of anticancer agent.

The encapsulation efficiency and loading content of PTX in the PLGA nanomedicine

To measure the PTX content in PTX-loaded PLGA nanomedicine, the NPs were diluted in acetonitrile. Subsequently, the concentration of PTX in samples was determined via a Waters Acquity UPLC apparatu equipped with a Waters Acquity UPLC HSS T3 (2.1 × 100 mm, 1.8 μm) chromatographic column. The mobile phase consisted of acetonitrile (A) and 0.1% formic acid (B). The gradient elution procedure was as follow: 0–19 min, 10%-95% (A); 19–20 min, 95%-100% (A); 20–21 min, 100%-10% (A); 21–25 min, 10%-10% (A); flow velocity 0.4 mL/min; column temperature 40°C; sample volume 2 μL. The monitoring wavelength range was 190–400 nm. The amount of PTX in PLGA nanomedicine was measured at 227 nm according to a standard curve (absorbance versus concentration). The PTX encapsulation efficiency was 13.7%, which was calculated as the ratio of the amount of PTX encapsulated in the NPs to the total amount of PTX fed for encapsulation. The PTX loading content in the PLGA nanomedicine was 5.5%, which was calculated as the ratio of the amount of PTX encapsulated in the NPs to the total amount of NPs including PTX.

Nanoparticle characterization

Both TEM (transmission electron microscope) and DLS (dynamic light scatterer) were used to characterize the PLGA NPs. Aliquots of PLGA NP suspension were firstly dispensed onto sheets of parafilm in a humidified petri dish and the vesicles were deposited on a carbon-coated grid (300-mesh) for 3 min. Subsequently, the grids were analyzed using a transmission electron microscope (JEM-1230, JEOL). While analysis of particle size distribution was performed by a dynamic light scatterer (Malvern ZetaSizer Nano ZS90).

Stimuli response of NR-loaded PLGA nanomedicine

NR-loaded nanomedicine was used to perform the controlled release of the PLGA nanomedicine, because NR not only possesses red fluorescence but also is hydrophobic like PTX [22]. First, 7.5 mg of NR-loaded PLGA nanomedicine was dissolved in 7.5 ml of 1 × PBS buffer (pH = 7.4), and divided into 15 portions in 500 μl. Then 500 μl of water, 10 mM or 20 mM of r-GSH was added to five of them used as control, 5 mM

and 10 mM groups, respectively. Finally, three samples from different groups were precipitated at predetermined time intervals, and the content of NR in supernatant was determined by an ultraviolet spectrophotometer at 551 nm.

Cell culture and cell viability assay

The LLC (Lewis lung carcinoma cell) cell line was purchased from the Cell Center of Chinese Academy of Medical Sciences. The cells were cultured in DF12 medium (Gibco, USA) with 10% fetal bovine serum (Biological Industries, Israel) and incubated at 37 °C in a humidified air containing 5% CO_2.

The CTC-TJH-01 (circulating tumor cell) cell line was isolated from the peripheral blood of patients with stage II lung cancer [26]. The 16HBE (Human bronchial epithelial cell) cell line was purchased from the Cell Center of Chinese Academy of Medical Sciences. The cells were cultured in F12K medium (Gibco, USA) with 10% fetal bovine serum (Biological Industries, Israel) and incubated at 37 °C in a humidified air containing 5% CO_2.

Targeted effect of FA modified nanomedicine

For analysis of the targeted effect of FA using flow cytometry, human bronchial epithelial cell 16HBE, lung cancer cell LLC and CTC were firstly seeded in 6-well plates with 2×10^5 cells per well and cultured for 24 hours. Then the cells were incubated with 0.5 mg/ml of NR-loaded FA-modified PLGA nanomedicine for 4 hours. Finally, the cells were harvested and analyzed on a flow cytometer (BD) at the PE (red) channel.

For analysis of the targeted effect of FA using fluorescence microscope, human bronchial epithelial cell 16HBE, lung cancer cell LLC and CTC were firstly seeded in confocal dishes with 2×10^5 cells per well and cultured for 24 hours. Then, the abovementioned cells were incubated with 0.5 mg/ml of NR-loaded FA-modified PLGA nanomedicine for 4 hours. Subsequently, the samples were washed with PBS and fixed with 4% paraformaldehyde for 30 min. And 0.5 μg/ml of Hoechst 33258 was used to stain the cell nucleuses for 5 minutes after washing with PBS. Finally, the targeted effect of FA was observed by a fluorescence microscope (Leica) at the red channel after washing with double distilled water and dry.

In vitro anti-tumor efficacy of PLGA nanomedicine in lung cancer cells

As for the biocompatibility analysis of blank NPs or cell viability assay, human bronchial epithelial 16HBE cells, lung cancer LLC and CTC cells were seeded in 96-well plates with 2×10^3 cells per well in quadruplicate, and cultured overnight. After incubation with different reagents for 48 hours, the cells were treated with a Cell Counting Kit-8 assay according to the manufacturer's specifications.

For apoptosis analysis, lung cancer LLC and CTC cells were firstly seeded in 6-well plates (2×10^5 per/well) and cultured for 24 hours. Then the cells were incubated with 5 nM of free PTX or its nanomedicine for 48 hours. Then the cells were harvested and resuspended in Annexin V binding buffer,

and stained with Annexin V-FITC and PI at 37 ℃ for 5 minutes. Finally, the cells were analyzed on the flow cytometer.

In vivo **antitumor efficacy of PLGA nanomedicine.**

To establish xenograft tumor, six-week old male C57 mice (about 20 g) purchased from Lingchang Biological Technology (Shanghai, China) were divided into four groups randomly (each group n = 6). Then subcutaneously injected with 5×10^5 of LLC cells on left side of the armpit of each mouse. The length and width of tumors were measured by calipers twice a week, and the tumor volume was calculated as (length × width^2)/2.

To evaluate the anticancer activity of the nanomedicine *in vivo*, the mice were intraperitoneally injected with saline, blank NPs, free PTX (10 mg/kg), PTX-loaded nanomedicine (at a PTX dose of 10 mg/kg) and treated every 3 days after the tumor volume reached approximately 50 mm^3. All mice were sacrificed and their tumor weights and gross volumes were measured when the largest tumor volume reached approximately 1000 mm^3. In addition, orbital blood obtained before mice sacrifice was mainly used for the detection of hepatorenal function. And the tumor tissues were fixed in 4% paraformaldehyde solution for the immunohistochemical analysis.

Immunohistochemical staining

First, tumors in each group were fixed with 5 ml of formalin overnight, dehydrated in ethanol, embedded in paraffin and sectioned (5 μm). Second, slides were then deparaffinized in xylene and ethanol, and rehydrated in water. Third, antigen retrieval was performed by heating in a microwave for 30 minutes in sodium citrate buffer (pH 6.0). Then, slides were quenched in hydrogen peroxide (3%) to block endogenous peroxidase activity and washed with TBST buffer. Finally, the primary antibodies were incubated at 4 ℃ overnight followed by using the SuperPicture™ Polymer Detection kit (Life Technologies) according to the manufacturer's instructions as described, and antibodies against cleaved caspase 3 (Abcam) and Ki-67 (Abcam) were used.

Statistical analysis

Statistical analysis was given as the means ± standard deviations (SD). Moreover, statistically significant difference between two groups was analyzed by hypothesis testing with the Two-Sample t Test, and indicated by * $p < 0.05$, ** $p < 0.01$, and *** $p < 0.001$, and $p < 0.05$ was considered statistically significant in all analyses (95% confidence level).

Results And Discussion

Smart responsive PTX-loaded FA-modified PLGA nanomedicine for the treatment of lung cancer

In order to improve the therapeutic efficacy and reduce the toxic side effects of anticancer agent PTX, stimuli responsive and targeted molecule modified organic nanomedicine was developed. As for the synthesis of NPs, biodegradable PLGA-SS-PEG-FA polymer was firstly prepared via a polymerization process. Subsequently, anticancer agent-loaded PLGA nanomedicine was synthetized by a facile solvent evaporation approach. As shown in Fig. 1, the delivery process of nanomedicine can be observed. First, FA modified nanomedicine was recognized by FR high-expressed tumor cells. Then, the nanomedicine was delivered into cytoplasm by endosome via FA and its receptor mediated endocytosis. After endosome-lysosome fusion, the nanomedicine was delivered into cytoplasm through lysosomes escape. Finally, the PLGA nanomedicine was stimulated by intracellular high GSH level, and anticancer agent was released for inhibiting the proliferation of lung tumor cells.

Synthesis and characterization of PLGA nanoparticles

The polymer PLGA-SS-PEG-FA was firstly synthesized through a four-step reaction, and the obtained product was measured by NMR (nuclear magnetic resonance). As shown in **Figure S1** (Supporting Information), the 1H NMR spectrum clearly demonstrated the presence of the different compounds corresponding to the proton peak at 1, 2, 3 and 4. The result indicated a successful synthesis of the PLGA-SS-PEG-FA copolymer.

Solvent evaporation approach was used to prepare the PLGA NPs. During the reaction, the mixture quickly turned from colorless into a milky white, indicating the formation of the PLGA NPs. In order to evaluate the morphology and the size of the PLGA NPs, transmission electron microscopy (TEM) and dynamic light scattering (DLS) were used. As shown in Fig. 2A, the TEM image demonstrated that the PLGA NPs possesses a spherical and uniform morphology with a diameter of around 150 nm. As shown in Fig. 2B, the DLS image is agreed well with the TEM result, and the size of most NPs are approximately 150 nm.

Biocompatibility of the PLGA nanoparticles

To guarantee the biocompatibility of the nano-carrier, PLGA was chosed as the basic composition. Biodegradable PLGA has approved as pharmaceutic adjuvant by FDA (Food and Drug Administration) Certification [27]. The degradation products of PLGA are lactic acid and glycolic acid, which are also the body's normal metabolic intermediate. As for PEG modification, it not only increases the water solubility and the elimination half-life of anticancer drugs, but also reduces the immunogenicity of chemotherapy agents. Therefore, the blank PLGA NPs should have the excellent biocompatibility in theory. As shown in **Figure S2** (Supporting Information), blank PLGA NPs has no obvious cytotoxicity to normal lung 16HBE cells and lung cancer LLC as well as CTC cells, indicating the PLGA NPs have admirable biocompatibility.

Controlled release triggered by GSH

Nowadays, many scientists are increasingly interested in construction the nanomedicine with smart response at tumor microenvironment, especially like GSH stimuli. The reason is that the concentration of GSH in cytosol of cancer cells (~ 2–10 mM) is significantly higher than that of extracellular matrix and blood (~ 2–20 μM) [28]. Importantly, there are usually higher GSH levels in tumor cells than these in

normal cells [29]. As shown in Fig. 3A, the concentration of GSH in lung cancer LLC and CTC cells are over 3-fold higher than that of lung normal 16HBE cells. For exploring GSH-responsive property, NR-loaded PLGA nanomedicine were treated with 5 mM and 10 mM of reduced GSH to observe the controlled release behavior due to the optical signal of NR [22]. As shown in Fig. 3B, the NR release curve showed that only 12% drug release was observed in the control group. We speculated that the minor release of NR was caused by the excellent stability of the PLGA nanocarrier under normal condition. While the drug release reached up to 41% and 73% after treating with 5 mM and 10 mM of GSH within 12 h, respectively. It's mainly due to the disulfide-bond breakage in a reductive manner, and the release of the cargo. Moreover, most of anticancer agent is released from the PLGA nanomedicine during the first 3 hours. These results confirmed that the PLGA nanomedicine could respond to GSH and trigger the on-demand drug release correspondingly.

Targeted delivery of FA

For verifying the targeted effect of FA, FA modified NR loaded PLGA nanomedicine was incubated with human bronchial epithelial 16HBE cells, lung cancer LLC and CTC cells for 4 hours. As depicted in Fig. 4A, flow cytometry analysis indicated that there is a small amount of PLGA nanomedicine around lung normal 16HBE cells. The right shift in 16HBE cells might be due to a nonspecific adsorption, like fluorescence microscopy image of 16HBE cells in Fig. 4B. In contrast, there are a large amount of targeted adsorption of the nanomedicine around lung cancer LLC and CTC cells, suggesting the excellent targeted effect of FA in tumor cells. As shown in Fig. 4B, fluorescence microscopy images are consistent well with the results of flow cytometry. These data demonstrated that the modification of FA as the targeted molecule on the surface of nanomedicine can deliver anticancer drug specifically to tumor cells.

In vitro **inhibitory efficacy of PLGA nanomedicine on lung cancer cells**

For exploring the anticancer effect of the PLGA nanomedicine, nanomedicine containing different concentrations of PTX were incubated with lung cancer cells for 48 hours, and free PTX was used as the control group. As shown in Fig. 5A, the half maximal inhibitory concentration (IC50) of free PTX is 24 nM in LLC cells. While the IC50 of PTX-loaded nanomedicine is only 4 nM, which is six times lower, indicating that the PLGA nanomedicine has the better inhibiting ability compared with its free anticancer agent in lung LLC cells. Moreover, apoptosis analysis was also performed to confirm the anticancer effect of the nanomedicine. As shown in Fig. 5B and 5C, the percentage of apoptosis in LLC cells increased to 19% after treating with 5 nM of free PTX for 48 hours. More attractively, the PLGA nanomedicine containing 5 nM of PTX induced 43% of cell apoptosis, revealing that the nanomedicine possesses the excellent ability for promoting apoptosis in lung LLC cells.

In the meantime, the inhibiting effects of the PLGA nanomedicine on lung cancer CTC cells were also performed. As shown in Fig. 6A, the IC50 of the nanomedicine is 2 nM. While the IC50 of free PTX reaches up to 6 nM, a 3-fold increase, indicating that the nanomedicine has the ability to suppress the proliferation of CTC cells greatly. As shown in Fig. 6B and 6C, free PTX and its nanomedicine can cause

7% and 18% of apoptosis ratio in CTC cells, suggesting that the nanomedicine can promote more CTC cells apoptosis than that of free PTX. These results indicated that the PLGA nanomedicine can effectively suppress proliferation and promote apoptosis of lung cancer cells. This might be due to the different ways of cell uptake for these agents. For example, the PLGA nanomedicine enters cells via endocytosis whereas free PTX through diffusion. In this aspect, endocytosis seemed more efficient for carrying high amount of PTX in contrast to simple diffusion through cell membrane [30]. Importantly, the PLGA nanomedicine posed much higher selective cytotoxicity to FR high expressed and GSH-elevated lung cancer cells than that to normal cells. All the observations demonstrated that the PLGA nanomedicine has the better therapeutic effect than that of free PTX for the treatment of lung cancer.

In vivo **antitumor activities of the PLGA nanomedicine**

In vivo antitumor efficacy of the PLGA nanomedicine was further investigated in nude mice with LLC cell xenograft tumor model. The tumor-bearing mice (~ 100 mm^3) were randomly divided into four groups with six mice in each group. Then one of the groups was separately treated with saline, blank PLGA NPs, free PTX or PTX-loaded nanomedicine through intraperitoneal injection every third day. Before each treatment, the tumor volume and body weight were recorded. As shown in Fig. 7A, the tumor volume of saline group gradually grew larger as times went on. And the tendency of blank PLGA NPs group was similar as the control group, indicating the admirable biocompatibility of the PLGA nanocarrier. A relative slowly growth was observed for free PTX. In contrast, the PLGA nanomedicine almost suppressed the growth of subcutaneous tumors, revealing that the PLGA nanomedicine has the better therapeutic efficacy than that of free PTX. Additionally, as shown in Fig. 7B, neither mouse death nor significant drop in body weight was observed in any groups during the therapy, suggesting that the experimental treatments were well tolerated. This may be due to the small dose of anticancer agent and the long treatment interval in the process of therapy. As shown in Fig. 7C and 7D, the tumor photo and the tumor weight clearly showed that both free PTX and its nanomedicine could effectively inhibit tumor growth, with the inhibition rate of 41% and 73% on the 21th day, respectively. These results revealed that the PLGA nanomedicine has the best inhibiting ability in tumor development, and this is probably due to the enhanced permeability and retention effect of the targeted delivery and GSH stimuli of the PLGA nanomedicine in tumor vasculature.

Immunohistochemical results were also obtained to observe the anticancer efficacy of the PLGA nanomedicine. As shown in Fig. 8, compared with the control group, the blank PLGA NPs have the similar results of tumor proliferation factors (Ki-67) and apoptosis factors (cleaved caspase-3). Free PTX possesses the significantly increased positive staining of cleaved caspase-3 and dramatically reduced positive staining of Ki-67. Notably, the PLGA nanomedicine has the most positive staining of cleaved caspase-3 and fewest positive staining of Ki-67, suggesting the PLGA nanomedicine possesses the better curative effect compared with free anticancer agent. All these results revealed that targeted delivery and smart response in tumor microenvironment contributed to an excellent antitumor activity of the PLGA nanomedicine.

Hepatorenal toxicity of the PLGA nanomedicine

The hepatorenal toxicity of the PLGA nanomedicine was further evaluated, such as ALT (alanine amino transaminase) and AST (aspartate transaminase) for liver function indicators, and CRE (creatinine) for renal function indicator. As shown in Fig. 9, the ALT, AST and CRE levels of the mice treated with free PTX indicated obvious side effects. However, PTX loaded nanomedicine had less influence on the hepatorenal function of mice compared with that of free PTX, indicating the PLGA nanomedicine has less toxic side effects in the treatment of lung cancer. These results probably be ascribed to the on-demand drug release triggered from the PLGA nanomedicine by the higher GSH level in tumor environment.

Conclusion

A targeted molecule modified smart responsive biodegradable PLGA nanomedicine was designed for improving the therapeutic effect of anticancer agent. The PLGA nanomedicine can be recognized and endocytosed by tumor cells through FA and its receptor mediated cellular endocytosis. The higher level of GSH in tumor microenvironment could lead to on-demand cargo release. *In vitro* and *in vivo* experiments indicated that the PLGA nanomedicine can inhibit proliferation and promote apoptosis of lung tumor cells, and has better therapeutic efficacy and less toxic side effects than that of free anticancer drug. This nanomedicine delivery platform is biocompatible and biodegradable, with the byproducts being lactic acid and glycolic acid. Importantly, other chemotherapeutic agents or genes might also be selectively delivered by this smart responsive nano-carrier. Furthermore, this design affords a nanoplatform for anti-cancer therapy with high efficacy and low toxicity whether it's one medicine or a combination of multiple medicines. Therefore, the proposed drug delivery system represents high promise as a future powerful treatment tool for effective therapies of various types of malignant tumors.

Declarations

Ethics approval and consent to participate

All institutional and national guidelines for the care and use of animals were followed.

Competing interests

The authors declare that they have no competing interests.

Consent for publication

All authors have read this manuscript and approved it for publication.

Acknowledgements

This work was supported by the National Natural Science Foundation of China (81774166, 81803777, 81973517, 81572949 and 31500696), Excellent Academic Leaders of Health and Family Planning

System in Shanghai (2017BR044).

References

1. Siegel RL, Miller KD, Jemal A. Cancer statistics, 2019. CA Cancer J Clin. 2019;69:7–34.
2. Siegel RL, Miller KD, Jemal A. Cancer statistics, 2020. CA Cancer J Clin. 2020;70:7–30.
3. Lemjabbar-Alaoui H, Hassan OU, Yang YW, Buchanan P. Lung cancer: biology and treatment options. Biochim Biophys Acta. 2015;1856:189–210.
4. Ishiguro K, Zhu YL, Lin ZP, Penketh PG, Shyam K, Zhu R, et al. Cataloging antineoplastic agents according to their effectiveness against platinum-resistant and platinum-sensitive ovarian carcinoma cell lines. J Transl Sci. 2016;2:117–24.
5. Adrianzen Herrera D, Ashai N, Perez-Soler R, Cheng H. Nanoparticle albumin bound-paclitaxel for treatment of advanced non-small cell lung cancer: an evaluation of the clinical evidence. Expert Opin Pharmacother. 2019;20:95–102.
6. Abu Samaan TM, Samec M, Liskova A, Kubatka P, Büsselberg D. Paclitaxel's mechanistic and clinical effects on breast cancer. Biomolecules. 2019;9:789.
7. Kundranda MN, Niu J. Albumin-bound paclitaxel in solid tumors: clinical development and future directions. Drug Des Devel Ther. 2015;9:3767–77.
8. Blair HA, Deeks ED. Albumin-bound paclitaxel: a review in non-small cell lung cancer. Drugs. 2015;75:2017–24.
9. Zhao M, van Straten D, Broekman MLD, Preat V, Schiffelers RM. Nanocarrier-based drug combination therapy for glioblastoma. Theranostics. 2020;10:1355–72.
10. Baeza A. Tumor targeted nanocarriers for immunotherapy. Molecules. 2020;25:1508.
11. Gaitanis A, Staal S. Liposomal doxorubicin and nab-paclitaxel: nanoparticle cancer chemotherapy in current clinical use. Methods Mol Biol. 2010;624:385–92.
12. Shah NN, Merchant MS, Cole DE, Jayaprakash N, Bernstein D, Delbrook C, et al. Vincristine sulfate liposomes injection (VSLI, Marqibo(R)): results from a phase I study in children, adolescents, and young adults with refractory solid tumors or leukemias. Pediatr Blood Cancer. 2016;63:997–1005.
13. Hajebi S, Rabiee N, Bagherzadeh M, Ahmadi S, Rabiee M, Roghani-Mamaqani H, et al. Stimulus-responsive polymeric nanogels as smart drug delivery systems. Acta Biomater. 2019;92:1–18.
14. Danhier F. To exploit the tumor microenvironment: since the EPR effect fails in the clinic, what is the future of nanomedicine? J Control Release. 2016;244:108–21.
15. Carter T, Mulholland P, Chester K. Antibody-targeted nanoparticles for cancer treatment. Immunotherapy. 2016;8:941–58.
16. Zhang Z, Dong C, Yu G, Cheng W, Liang Y, Pan Y, et al. Smart and dual-targeted BSA nanomedicine with controllable release by high autolysosome levels. Colloids Surf B Biointerfaces. 2019;182:110325.

17. Zhang Z, Cheng W, Pan Y, Jia L. An anticancer agent-loaded PLGA nanomedicine with glutathione-response and targeted delivery for the treatment of lung cancer. J Mater Chem B. 2020;8:655–65.
18. Handali S, Moghimipour E, Rezaei M, Ramezani Z, Kouchak M, Amini M, et al. A novel 5-fluorouracil targeted delivery to colon cancer using folic acid conjugated liposomes. Biomed Pharmacother. 2018;108:1259–73.
19. Lee Y, Thompson DH. Stimuli-responsive liposomes for drug delivery. Wiley Interdiscip Rev Nanomed Nanobiotechnol 2017; 9: 10.1002/wnan.1450.
20. Zhang Z, Balogh D, Wang F, Sung SY, Nechushtai R, Willner I. Biocatalytic release of an anticancer drug from nucleic-acids-capped mesoporous SiO_2 Using DNA or molecular biomarkers as triggering stimuli. ACS Nano. 2013;7:8455–68.
21. Zhang Z, Balogh D, Wang F, Willner I. Smart mesoporous SiO_2 nanoparticles for the DNAzyme-induced multiplexed release of substrates. J Am Chem Soc. 2013;135:1934–40.
22. Chen D, Zhang G, Li R, Guan M, Wang X, Zou T, et al. Biodegradable, hydrogen peroxide, and glutathione dual responsive nanoparticles for potential programmable paclitaxel release. J Am Chem Soc. 2018;140:7373–76.
23. Bansal A, Simon MC. Glutathione metabolism in cancer progression and treatment resistance. J Cell Biol. 2018;217:2291–98.
24. Wang Y, Huang HY, Yang L, Zhang Z, Ji H. Cetuximab-modified mesoporous silica nano-medicine specifically targets EGFR-mutant lung cancer and overcomes drug resistance. Sci Rep. 2016;6:25468.
25. Wang L, Liu L, Dong B, Zhao H, Zhang M, Chen W, et al. Multi-stimuli-responsive biohybrid nanoparticles with cross-linked albumin coronae self-assembled by a polymer-protein biodynamer. Acta Biomater. 2017;54:259–70.
26. Que Z, Luo B, Zhou Z, Dong C, Jiang Y, Wang L, et al. Establishment and characterization of a patient-derived circulating lung tumor cell line in vitro and in vivo. Cancer Cell Int. 2019;19:21.
27. Khan I, Gothwal A, Sharma AK, Kesharwani P, Gupta L, Iyer AK, et al. PLGA nanoparticles and their versatile role in anticancer drug delivery. Crit Rev Ther Drug Carrier Syst. 2016;33:159–93.
28. Han X, Song X, Yu F, Chen L. A ratiometric fluorescent probe for imaging and quantifying anti-apoptotic effects of GSH under temperature stress. Chem Sci. 2017;8:6991–7002.
29. Chang TC, Chang MJ, Hsueh S. Glutathione concentration and distribution in cervical cancers and adjacent normal tissues. Gynecol Obstet Invest. 1993;36:52–5.
30. Zhang S, Gao H, Bao G. Physical principles of nanoparticle cellular endocytosis. ACS Nano. 2015;9:8655–71.

Figures

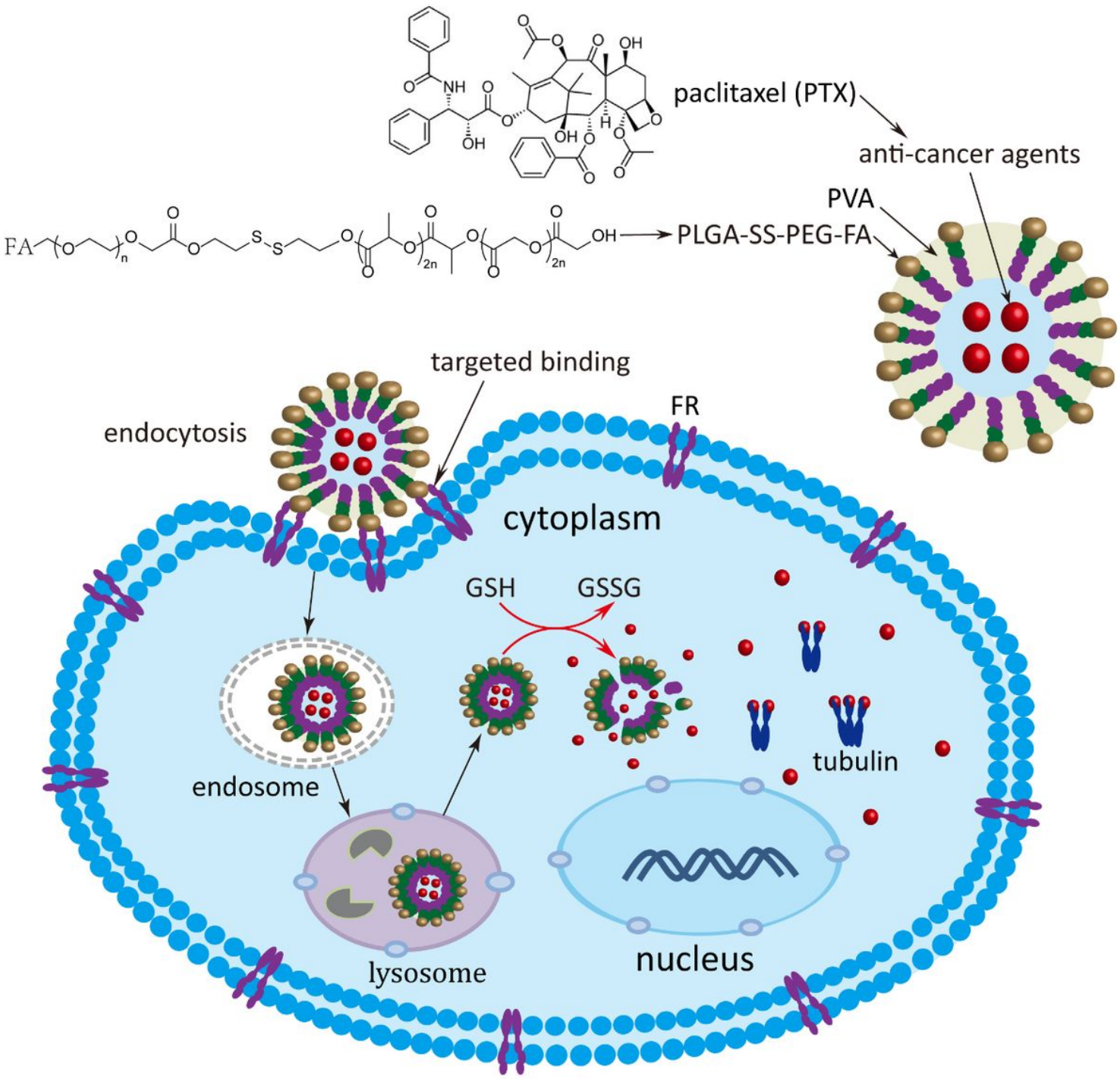

Figure 1

Schematic diagram of PTX nanomedicine with targeted delivery and smart response, paclitaxel (PTX), poly(vinyl alcohol) (PVA), poly(lactic-co-glycolic acid) (PLGA), polyethylene glycol (PEG), folic acid (FA), folate receptor (FR), GSH (glutathione).

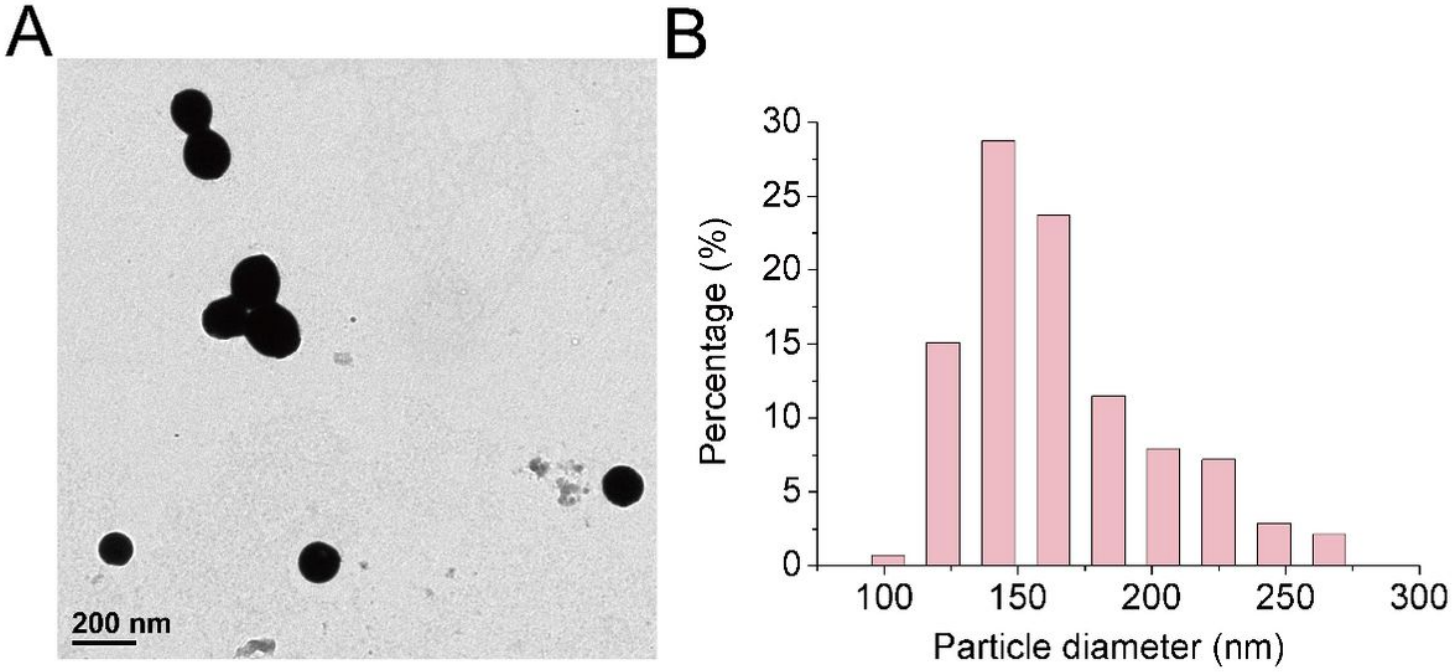

Figure 2

Characterization of synthesized PLGA NPs. (A) TEM image of PLGA NPs, scale bar: 200 nm. (B) Particle size distribution using a dynamic light scatterer.

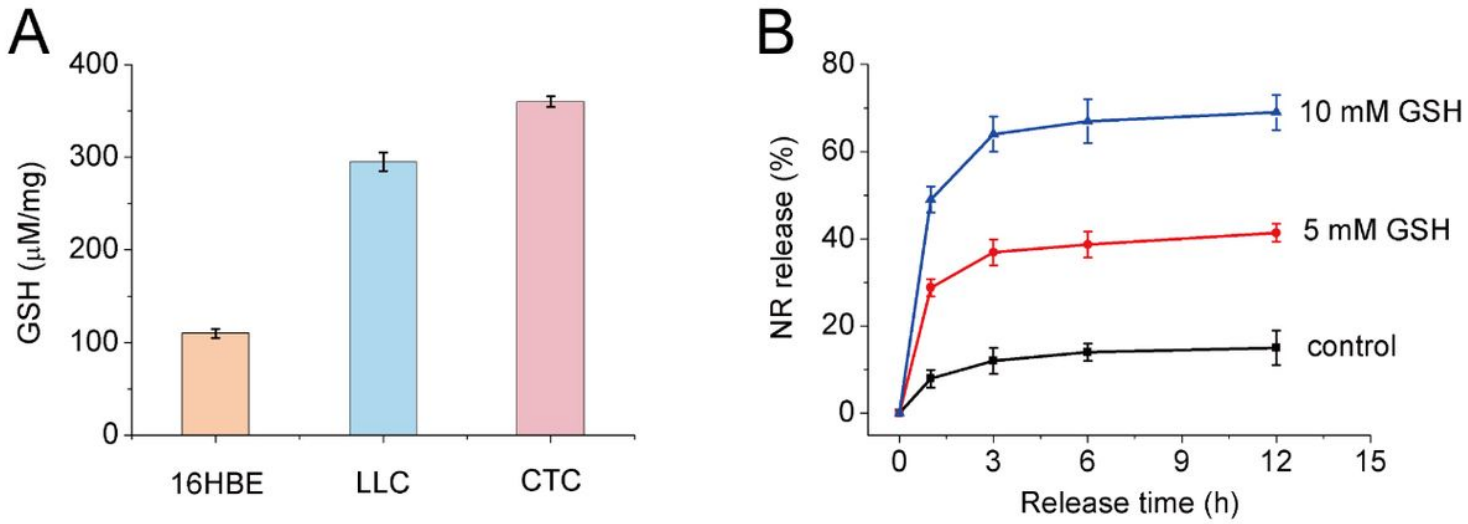

Figure 3

Controlled release of the PLGA nanomedicine. (A) GSH content in normal bronchial epithelial 16HBE, lung cancer LLC and CTC cells, error bars represent mean ± SD (standard deviation, n = 3). (B) NR release from NR-loaded PLGA-SS-PEG nanomedicine (0.5 mg/ml) after incubating with 5 mM and 10 mM of r-GSH in different time intervals, error bars represent mean ± SD (standard deviation, n = 3).

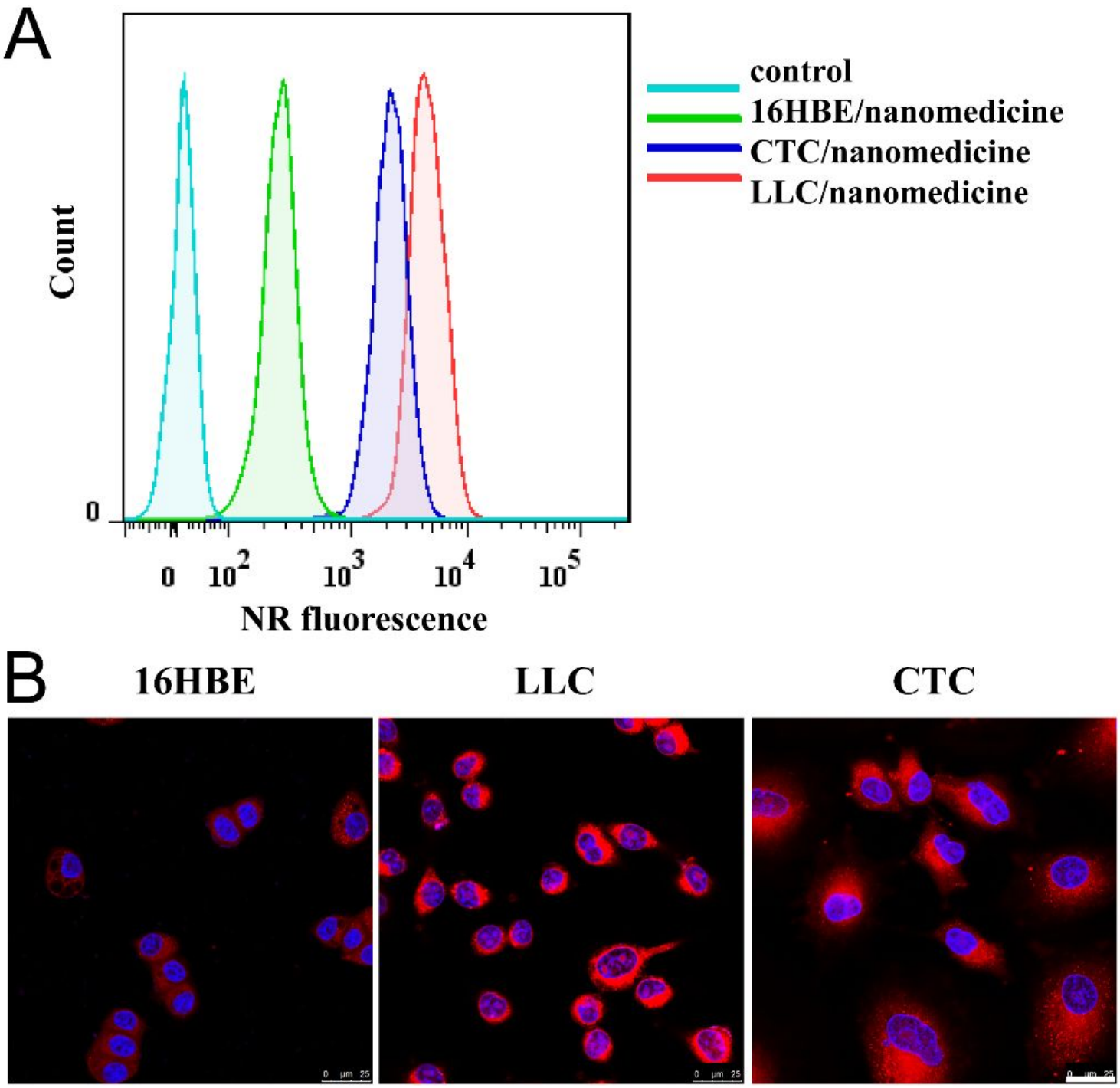

Figure 4

Targeted effect of FA modified NR loaded nanomedicine. (A) Flow cytometry (FACS) analysis of normal 16HBE, lung cancer LLC and CTC cells after treating with FA modified NR loaded nanomedicine (0.5 mg/ml) for 4 hours. (B) Fluorescence microscopy images, the red color is NR, the blue color is Hoechst, scale bar is 25 μm.

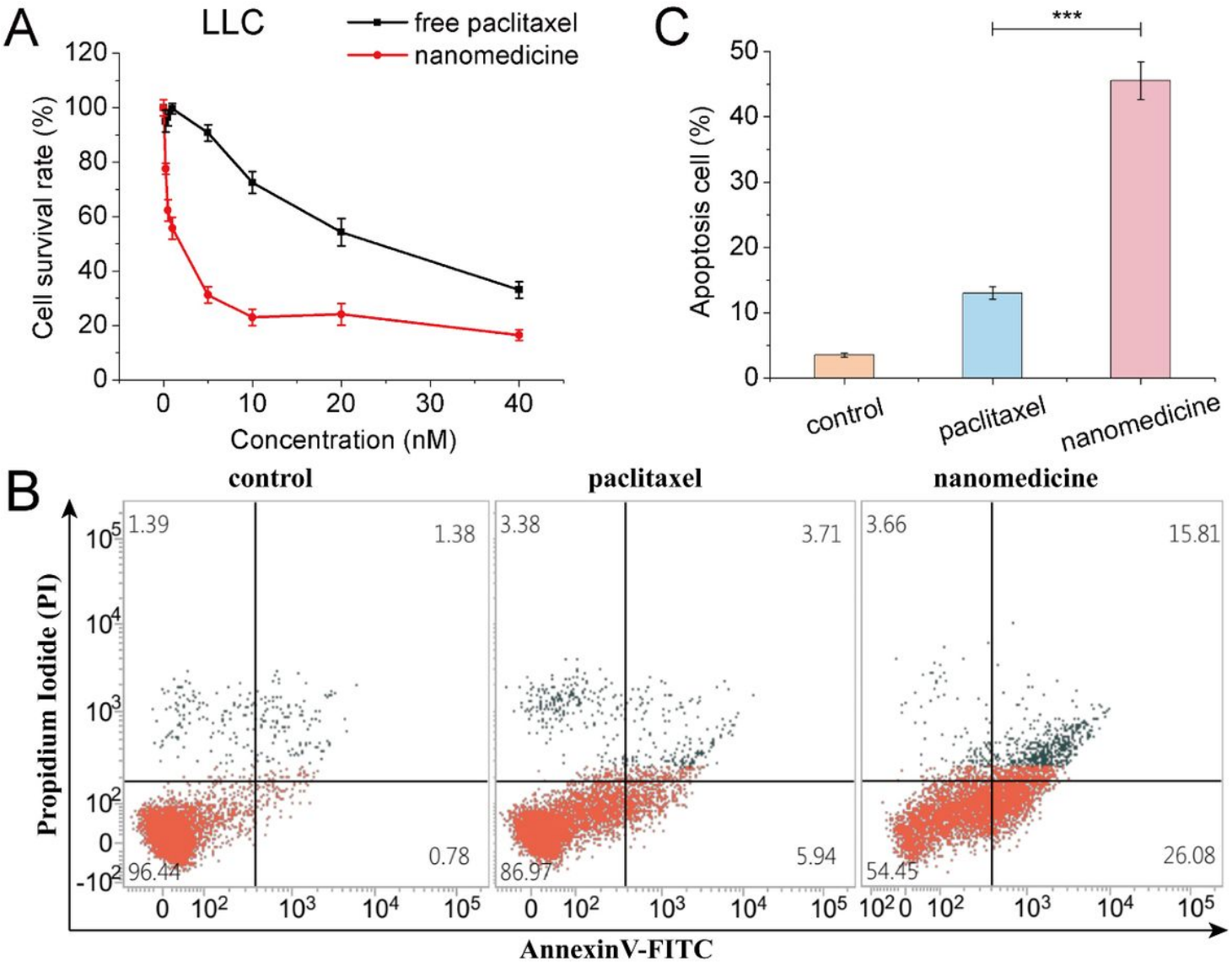

Figure 5

In vitro anti-tumor efficacy of PLGA nanomedicine in lung cancer LLC cells. (A) Viability of LLC cells after incubating with various concentrations of free PTX and its PLGA nanomedicine, error bars represent mean ± SD (standard deviation, n = 4). (B) Flow cytometric analysis of LLC cells after treating with 5 nM of PTX and its PLGA nanomedicine by Annexin V and FITC-PI staining. (C) Statistical analysis of apoptosis cells corresponding to (B), error bars represent mean ± SD (standard deviation, n = 3), **p< 0.01.

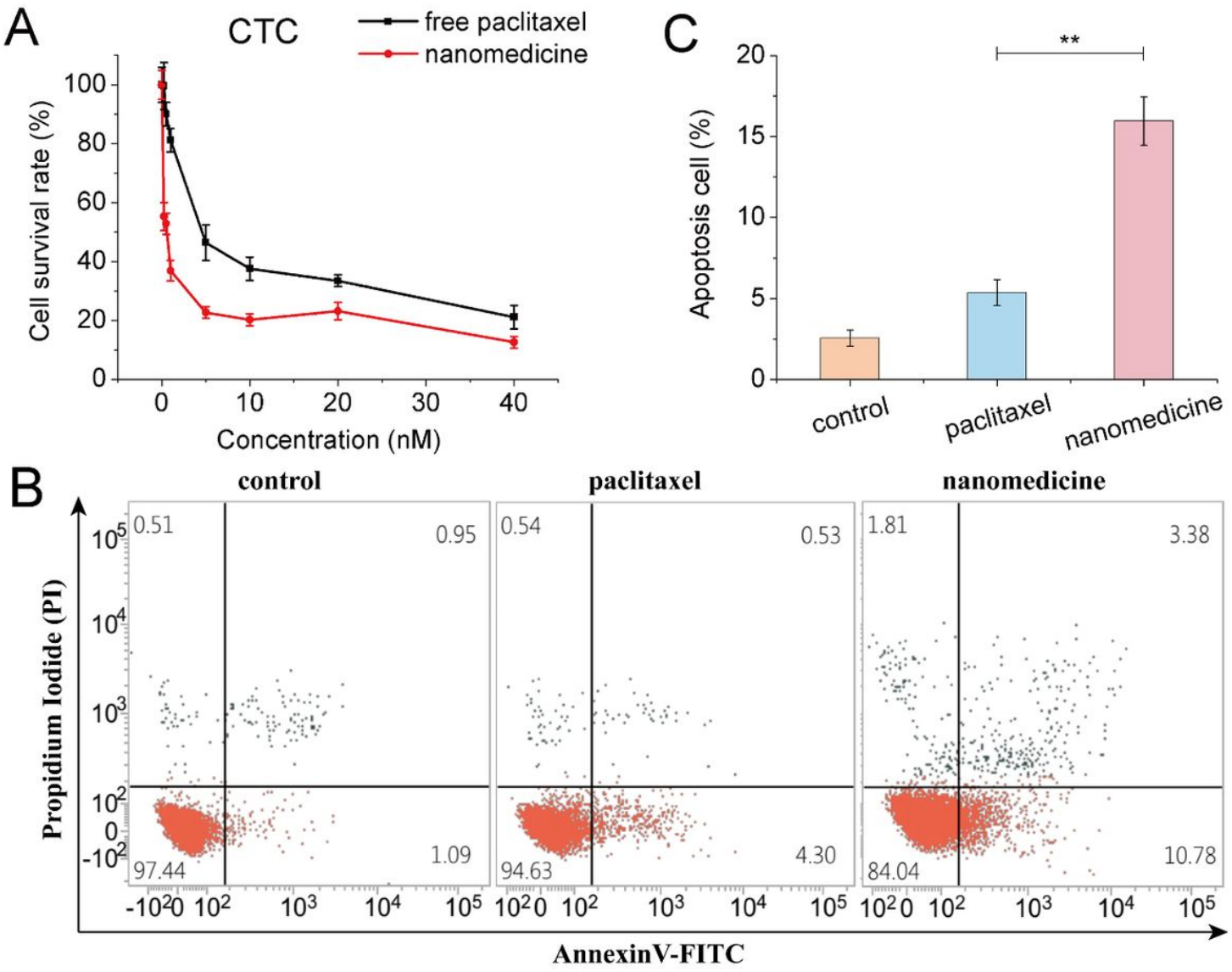

Figure 6

In vitro anti-tumor efficacy of PLGA nanomedicine in lung cancer CTC cells. (A) Viability of CTC cells after incubating with various concentrations of free PTX and its PLGA nanomedicine for 48 hours, error bars represent mean ± SD (standard deviation, n = 4). (B) Flow cytometric analysis of CTC cells after treating with 5 nM of PTX and its PLGA nanomedicine by Annexin V and FITC-PI staining. (C) Statistical analysis of apoptosis cells corresponding to (B), error bars represent mean ± SD (standard deviation, n = 3), **p< 0.01.

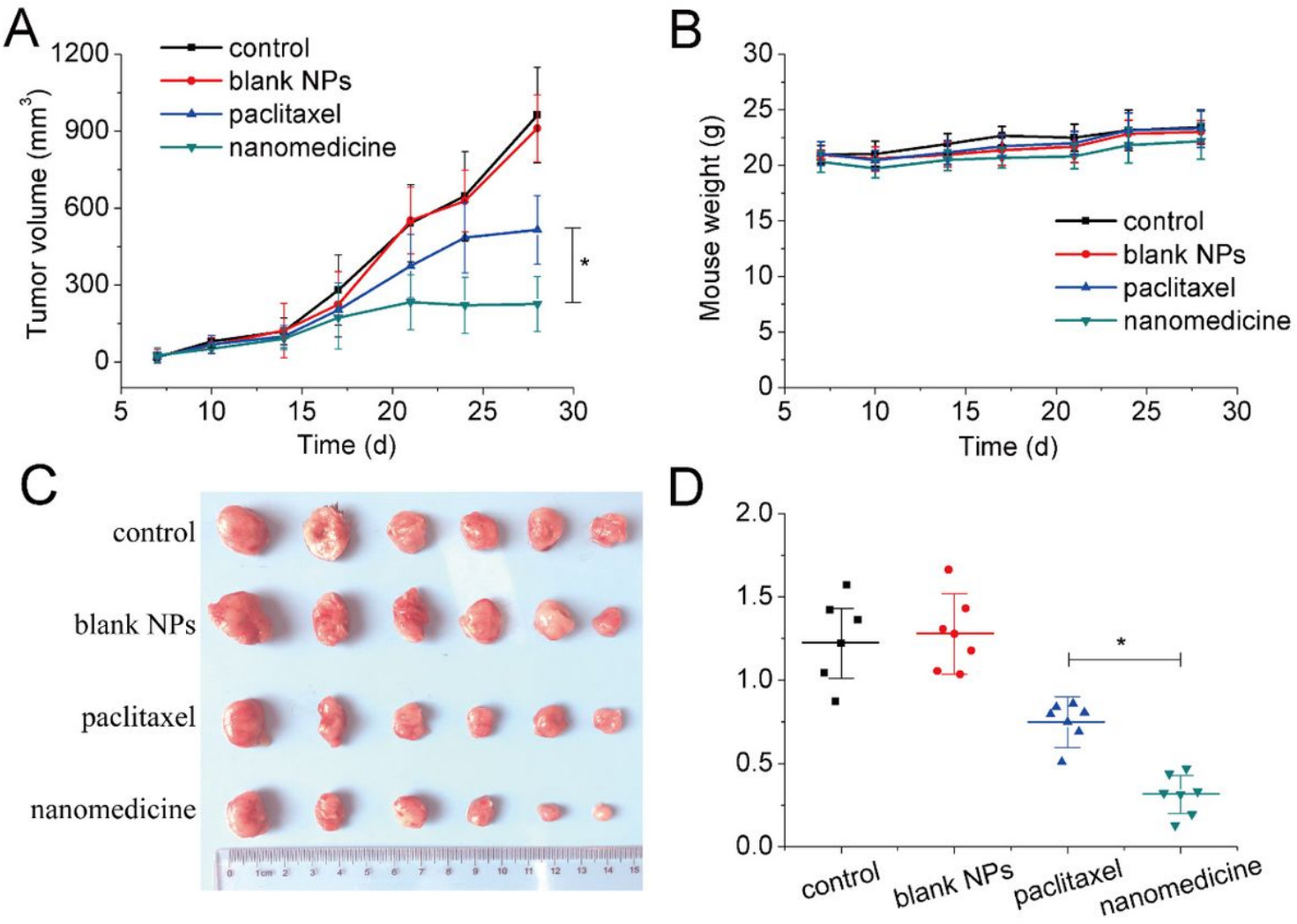

Figure 7

In vivo antitumor efficacy of PLGA nanomedicine. (A) Tumor volume growth curves, (B) body weights changes, (C) tumor photo and (D) tumor weight of LLC tumor bearing mice after systemic administration of saline, blank NPs, free PTX (10 mg/kg) and its PLGA nanomedicine (10 mg/kg of PTX), error bars represent mean ± SD (standard deviation, n = 6), *p< 0.05.

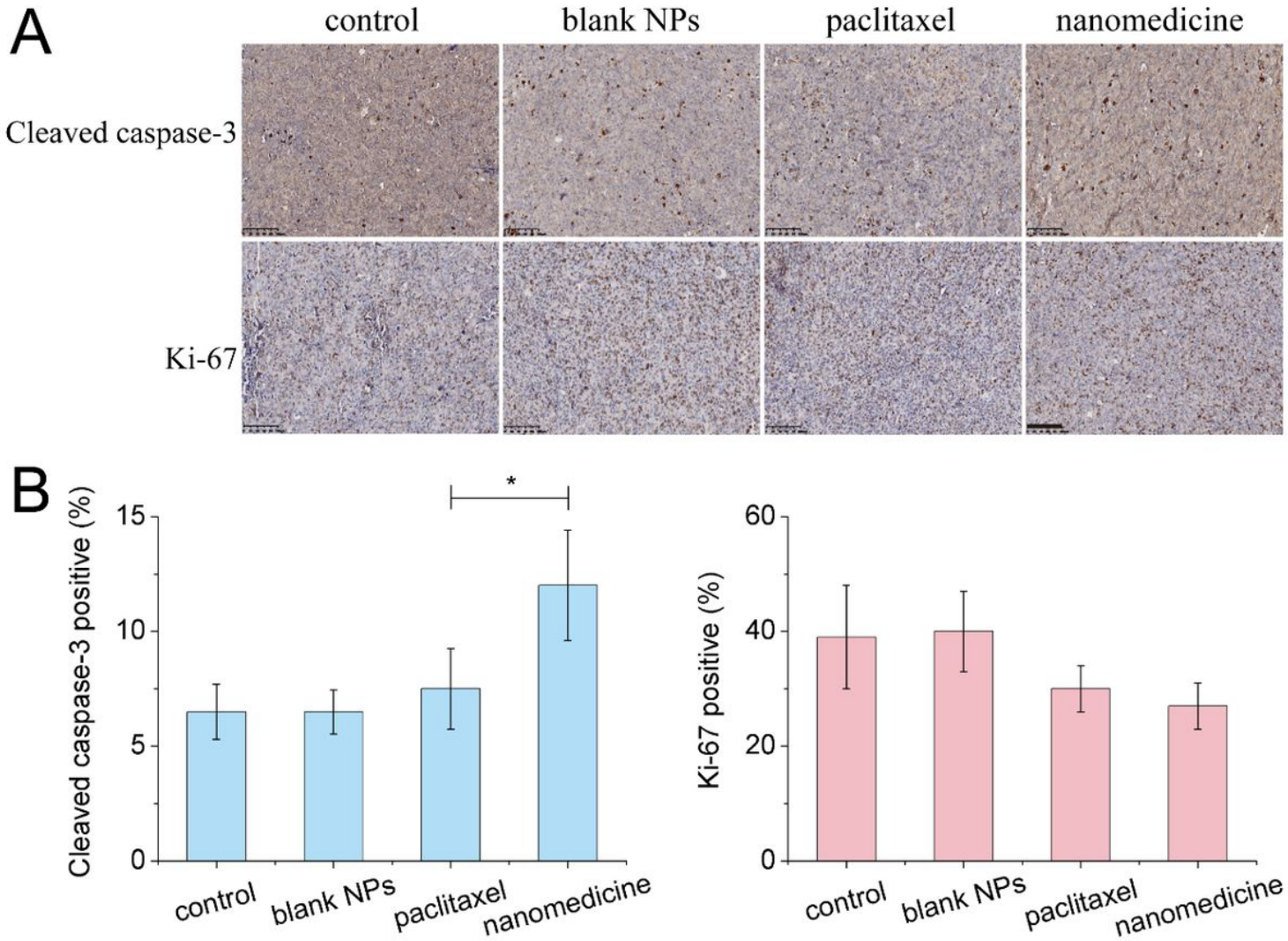

Figure 8

Immunohistochemical staining. (A) Cleaved caspase-3 and Ki-67 immunohistochemical staining of LLC tumor-bearing mice after systemic administration of saline, blank NPs, free PTX and its PLGA nanomedicine, scale bar is 100 mm. (B) Statistical analysis of immunohistochemical staining, error bars represent mean ±SD (standard deviation, n = 15), *p < 0.05.

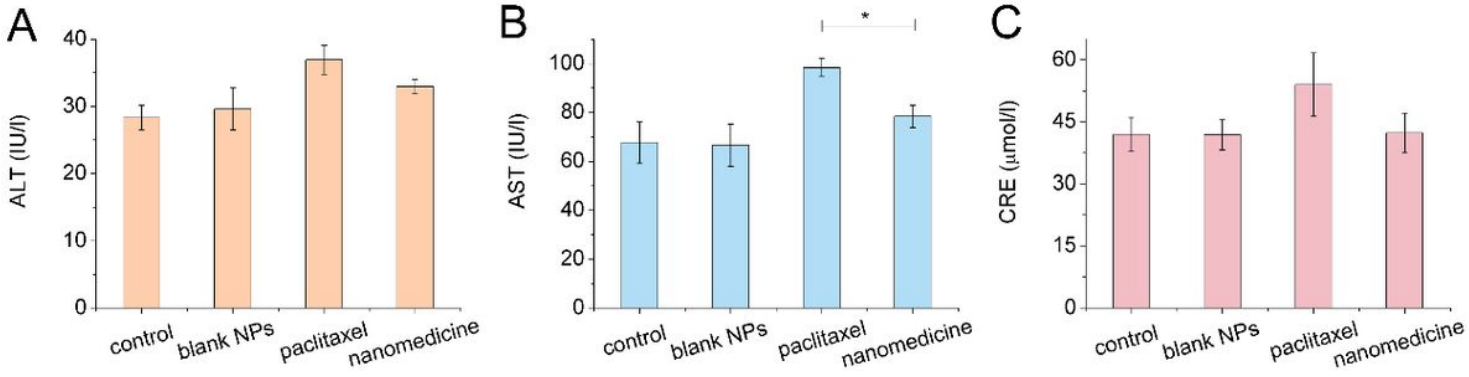

Figure 9

Changes in hepatorenal function indices. (A) AST (aspartate transaminase), (B) ALT (alanine transaminase) and CRE (creatinine) values when treated with saline, blank NPs, free PTX and its PLGA nanomedicine, where error bars represent mean ±SD (standard deviation, n = 3), *p < 0.05.

Supplementary Files

This is a list of supplementary files associated with this preprint. Click to download.

- SupportingInformation.docx
- SupportingInformation.docx
- SupportingInformation.docx